Forest Chemicals Review
www.forestchemicalsreview.com
ISSN: 1520-0191
July-August 2022 Page No. 788-802
Article History: Received: 30 March 2022, Revised: 8 April 2022, Accepted: 15 April 2022, Publication: 30 April 2022

Engineering Investigation of a Deepwater Turret Mooring Suction Pile Inverse Catenary Based on BV and DNVGL Rules

Xuanze Ju[1,2,3*], Zili Li[1,2], Baohui Dong[3], Jianghong Wang[3], Xianwu Meng[3]
[1] College of Pipeline and Civil Engineering, China University of Petroleum (East China), China
[2]Shandong Key Laboratory of Oil & Gas Storage and Transportation Safety, Qingdao, China
[3]Offshore Oil Engineering Co., Ltd., Engineering Company, Tianjin, China
*Corresponding Author.

Abstract:

FPSO is the key unit of deepwater oilfield development, but it needs to be highly reliable to resist the extreme offshore environment. In order to get a reliable engineering system, the engineering investigation of mooring suction pile inverse catenary is conducted. Base on the seabed data and its soil mechanics, a complete engineering mechanical model for inverse catenary of suction pile is established, in the meanwhile, proposed a mooring slack calculation method. The engineering of the inverse catenary and mooring slack was evaluated based on the mooring load conditions classified by BV and DNVGL requirements, the seabed loads derived from mooring analysis results. The investigation results show that in the design and checking conditions, the tension range of the suction pile inverse catenary of this FPSO mooring is 10254kN~14075kN, the lug load angle range is 16.2°~30.1°, and the horizontal projection distance of the embedded chain range is 47.33m~80.30m. It can also be seen that the calculation results of BV rule and DNV rule are relatively close, the results based on different rules are mutually verified. The calculated slack (movement of chain along seabed from pretension to max intact load) is expected to be in the range 2.3 m - 0.4 m dependent on soft or stiff soil conditions and on installation (pretension) load. The final results were applied in the most deepwater FPSO project in the South China Sea with a depth of 420 meters.

Keywords*: Offshore floating structure, Turret mooring system, Suction pile, Inverse Catenary.*

I. INTRODUCTION

A floating production storage and offloading unit (FPSO) is a floating vessel used by the offshore oil and gas industry for the production and processing of hydrocarbons, and for the storage of oil [1]. An FPSO vessel is designed to receive hydrocarbons produced by itself or from nearby platforms or subsea template, process them, and store oil until it can be offloaded onto a tanker or, less frequently, transported through a pipeline [2], illustrated as Fig 1 [3, 4]. Until now, the number and gross tonnage of China's FPSO ranks among the top in the world, and FPSO supports 80% of China's offshore oil production capacity, known as China's “Offshore Oil Fleet” [5]. China's largest offshore oil and gas developer,

Forest Chemicals Review
www.forestchemicalsreview.com
ISSN: 1520-0191
July-August 2022 Page No. 788-802
Article History: Received: 30 March 2022, Revised: 8 April 2022, Accepted: 15 April 2022, Publication: 30 April 2022

CNOOC, currently has 18 FPSOs with storage capacity of 350 to 2,000 thousand barrels and application water depth from 20 to 400 meters [6-8].

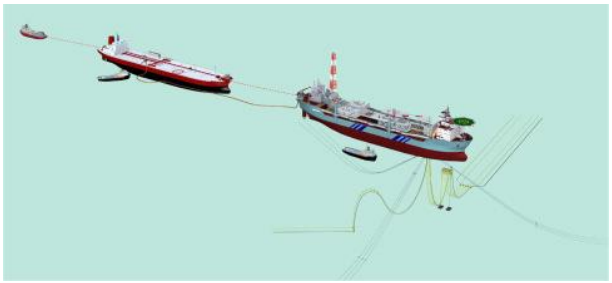

Fig 1: Turret moored FPSO with a shuttle tanker

The mooring line catenary configuration is the most common mooring system in water with a depth less than l500m [9], which consists of a group of lines combined of chain and wire rope. The restoring force of catenary mooring system is mainly provided by its own weight. There is enough length of mooring line resting on the seabed to avoid the anchor bearing vertical load. The full range of mooring anchor concepts including driven, suction, drilled and grouted, drag embedment anchors (DEAs), vertically loaded anchors (VLAs) and suction embedded plate anchors (SEPLAs) [10]. Due to some of the advantages that favor the use of suction piles are their short installation times and better control on their positioning, suction piles are widely used as anchors for floating systems in the offshore oil and gas industry, from shallow to deepwater [11]. Fig 2 shows a 2D geometry of the catenary mooring configuration. The bottom chain connected to the mooring point of the suction pile will be embedded in the seabed together with the suction pile, and the embedded chain presented a state of reverse catenary due to the lateral support provided by the soil, as shown in Fig 3. The interaction between the anchor chain and the soil changes the load and angle transferred to the mooring suction pile, and ultimately affects the bearing capacity and possible failure mode of the mooring foundation.

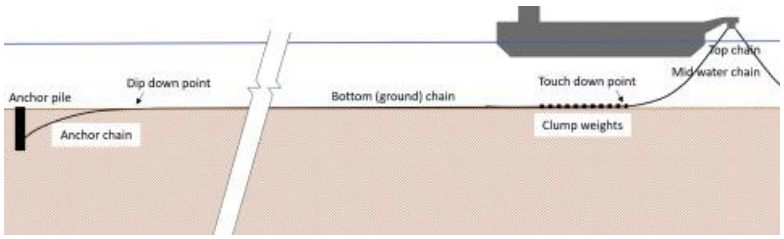

Fig 2: Catenary mooring configuration of a deepwater FPSO

Forest Chemicals Review
www.forestchemicalsreview.com
ISSN: 1520-0191
July-August 2022 Page No. 788-802
Article History: Received: 30 March 2022, Revised: 8 April 2022, Accepted: 15 April 2022, Publication: 30 April 2022

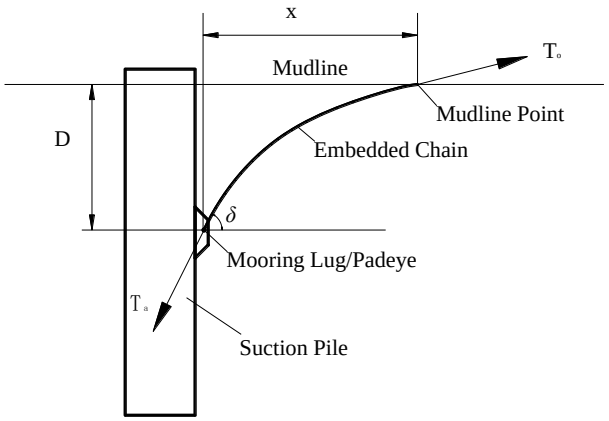

Fig 3: Embedded Chain Inverse Catenary Configuration for a deepwater mooring

There are three methods to study the inverse catenary track of embedded chain of mooring pile in soil including experimental method, analytical method and numerical method. (1) In terms of experimental research, Degenkamp and Dutta [12, 13] carried out experiments on three mooring lines with different diameters and a series of model tests in two viscous seabed soils with different undrained shear strengths. In these tests, the mooring line displacement, horizontal drag force and the force component of the drag anchor at the mooring point are measured, the effects of soil resistance and shear strength on the mooring cable are studied, and the relationship between the mooring cable tension and displacement is also studied. In order to verify the accuracy of the inverse catenary equation of state, Neubecker and Randolph [14] conducted a soil model test in dense sandy soil, which adopted a similar method to Degenkamp and Dutta, but measured the morphology of the inverse catenary. (2) In terms of analytical method research, the most representative is the analytic solution of inverse catenary proposed by. The analytical solution form of towed anchor embedding trajectory is given through combining and using the anchor bearing capacity calculated by empirical parameters, and different analytical solutions are given, but not considering the dead weight of anchor plate. (3) In terms of numerical method research, the studying core point is on the limit balance method based on the numerical study of engineering geology. This method assumes that the drag anchor moves along parallel to the direction of the anchor plate, and calculates the rotation of the anchor plate through the moment balance increment method (consistent with the direction of mooring line tension). At any buried depth, the seabed soil resistance on anchor pile can be calculated by using standard bearing capacity model or empirical data. Until now, the main researchers of this method include Stewart, Neubecker, Randolph, Thorne, Dahlberg, etc [16-21]. Currently, the internationally recognized theoretical prediction method comes from the prediction method for embedding drag anchor proposed by Neubecker and Randolph [14]. Combining the property that the motion direction of anchor plate is consistent with the tangent direction of embedding trajectory, the equation related to drag angle and force at mooring point can be obtained directly. However, this method is only applicable to the cohesive soil whose undrained shear strength of seabed soil conforms to power exponent.

The objective of this study is to present the inverse catenary design methodology, analyze inverse

Forest Chemicals Review
www.forestchemicalsreview.com
ISSN: 1520-0191
July-August 2022 Page No. 788-802
Article History: Received: 30 March 2022, Revised: 8 April 2022, Accepted: 15 April 2022, Publication: 30 April 2022

catenary design for a suction pile applied in a deepwater FPSO mooring system, meanwhile, considering mooring seabed loads as per BV and DNVGL rules, which provide good engineering results for this project and direct experiences for similar projects in the South China Sea.

II. FPSO TURRET MOORING SYSTEM AND LOADS AT SEABED

2.1 Turret Mooring Analysis Setup

This FPSO mooring system is composed of 9 mooring lines gathered in 3 bundles of 3 legs. The anchoring system is symmetric with 120 degrees spacing between bundles in order to limit the excursion of the turret, approximately 5° between each anchoring leg of the individual bundles. The mudline point (MLP) radius is about 1200m (from turret center to MLP), each line will be anchored to the seabed by means of a suction pile. The mooring line runs along the seabed (i. e angle at MLP is equal to 0°), before following an inverse catenary trajectory to the pad eye of the suction anchor. An overview of the mooring layout is given in Fig. 4 and Fig. 5. The embedded chain characteristics considered in the design are summarized in TABLE I.

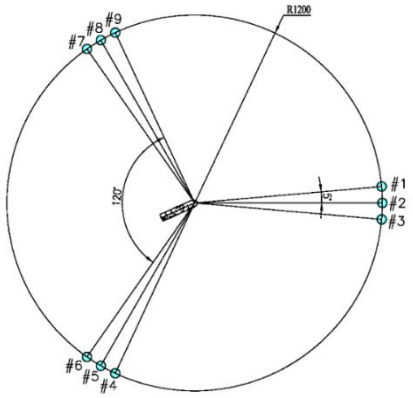

Fig 4: General layout of a deepwater FPSO mooring system

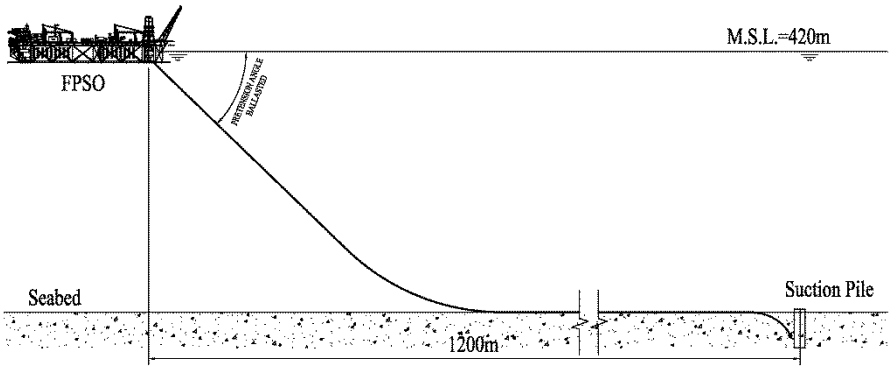

Fig 5: Turret mooring line for a deepwater FPSO

Forest Chemicals Review
www.forestchemicalsreview.com
ISSN: 1520-0191
July-August 2022 Page No. 788-802
Article History: Received: 30 March 2022, Revised: 8 April 2022, Accepted: 15 April 2022, Publication: 30 April 2022

TABLE I. Embedded Chain Characteristics

Chain Parameter	Unit	Value
Diameter	mm	160
Grade/Type	/	R3S
Weight in air	Kg/m	517.1
Weight in water	Kg/m	449.6
Minimum Breaking Load - New	kN	19,888
Minimum Breaking Load – Corroded	kN	17,154

2.2 3 Mooring loads at seabed

The mooring load at seabed shall be based on mooring analysis results, and its calculation method is the Mean of Maximum (or Mean of Minimum) as per over 30 random 3-hrs realizations (3-hour time domain simulations). Mooring lines and risers are subjected to current drag forces. These forces induce a mean horizontal pull on the FPSO. It is assumed that the direction of the pull is in the opposite direction of the current. Time domain analyses are conducted in view of evaluating mooring global performance against design criteria and constraints. The mooring system is designed to withstand a 100 yr (intact and damaged mooring line conditions) and 1000 yr (intact mooring line condition) tropical cyclone wave loading. Mooring system is also verified for a 100 yr seismic event under operational load condition (1 yr tropical cyclone load). The mooring system was designed to satisfy all the design cases required by BV [22] and DNVGL [23] standards. The design unfactored mooring line loads at MLP and corresponding partial load factors, according to both BV and DNVGL standards, are executed. The design factored mooring loads at MLP according to BV and DNVGL design cases are summarized in TABLE II and TABLE III, respectively. As shown in TABLE III, the “intact case 2” gives higher tension load than “intact case 1”. Conservatively, only “intact case 2” was considered for anchoring geotechnical design.

TABLE II. Design Load Conditions at MLP - BV

Design case	Mooring Condition	Return Period [yr]	Factored Mooring Load Td [kN]
Intact case 1	Intact	100	6,081
Intact case 2	Intact	100	10,847
Redundancy case	Damaged	100	11,440
Accidental case	Intact	1,000	12,165

Forest Chemicals Review
www.forestchemicalsreview.com
ISSN: 1520-0191
July-August 2022 Page No. 788-802
Article History: Received: 30 March 2022, Revised: 8 April 2022, Accepted: 15 April 2022, Publication: 30 April 2022

TABLE III. Design Load Conditions at MLP - DNVGL

Limit State	Mooring Condition	Return Period [yr]	Factored Mooring Load Td [kN]
ULS	Intact	100	12,593
ALS	Damaged	100	13,718
ALS	Intact	1,000	14,825
Sensitivity	Intact	1	4,570

III. SOIL PARAMETERS

3.1 Soil Set-Up and Adhesion Factors

Soil adhesion factors, considered for anchor design are shown in TABLE IV. The adhesion factor at 0 days (i.e. during anchor installation) was taken as 1/St. Adhesion factor values used for anchor retrieval (at both 1 and 7 days), holding capacity and removal (20 yrs) are based on site specific thixotropy tests performed for the project. In particular, Thixotropic characteristics of the clays were evaluated by conducting three series of miniature vane shear tests on samples from about 4.6 m to 26.4 m penetration, with six to eight tests per series, in order to study the strength set-up behavior with time. Interpreted average thixotropic strength gain profile was evaluated by means of the thixotropy test results and values of thixotropic strength ratio was derived for installation, retrieval, holding capacity and removal (Fig. 6).

TABLE IV. Pile-soil adhesion factors (α)

Case	Depth [m]	Thixotropic Strength Ratio [-]	Adhesion Factors, α[-]	
		S_A/S_R	Inside, α_{in}	Outside, α_{out}
Installation	0.0 - 4.8	1.00	0.42	
	4.8 – 16.0		0.45	
Retrieval (1 day)	0.0 - 4.8	1.18	0.49	
	4.8 - 16		0.54	
Retrieval (7 days)	0.0 - 4.8	1.41	0.59	
	4.8 – 16.0		0.64	
Holding capacity (30 days)	0.0 - 4.8	1.49	0.62	
	4.8 – 16.0		0.68	
Removal (20 yrs)	0.0 - 4.8	1.51	0.63	
	4.8 – 16.0		0.69	

Forest Chemicals Review
www.forestchemicalsreview.com
ISSN: 1520-0191
July-August 2022 Page No. 788-802
Article History: Received: 30 March 2022, Revised: 8 April 2022, Accepted: 15 April 2022, Publication: 30 April 2022

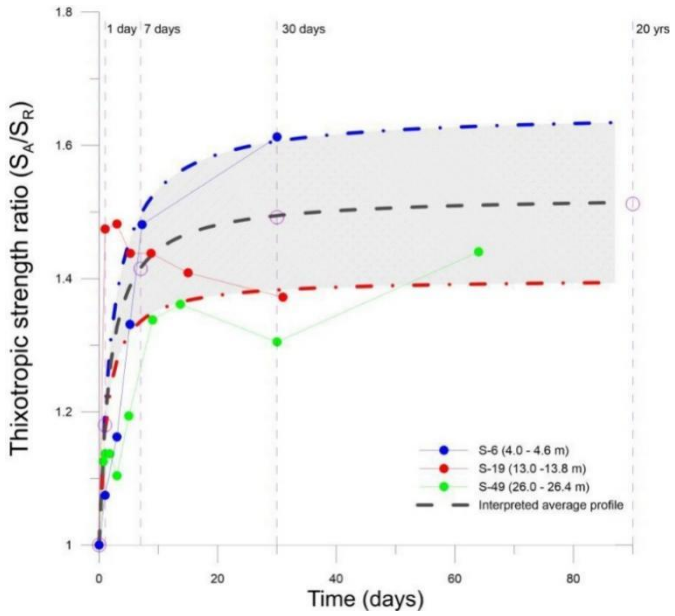

Fig 6: Interpreted average thixotropic strength gain profile

3.2 Design Soil Profiles

In order to consider the soil variability across the FPSO mooring area, the design undrained shear strength profiles were defined as envelopes of design profiles provided for the three-anchor cluster. In particular, lower and best estimate design profiles were derived as the lower envelope of the corresponding cluster design soil profiles, whereas the design upper estimate profile was derived as the upper envelope of anchor cluster design profiles. The design soil profiles in terms of undrained shear strength, total unit weight and soil sensitivity are summarized in TABLE V. The design total unit weight and undrained shear strength profiles are also graphically shown in Fig 7.

TABLE V. Design Soil Profiles

Depth [m]	Total Unit Weight γ[kN/m3]	Undrained Shear Strength, Su [kPa]			Sensitivity St[-]
		LE	BE	UE	
0.0	16.7	1.0	1.5	8.0	2.4
0.4		2.0	2.5	18.0	
0.4		5.0	7.0	18.0	
2.6		15.5	18.0	25.0	
4.8		17.2	20.9	32.0	
4.8	17.1	17.2	20.9	32.0	2.2

Forest Chemicals Review
www.forestchemicalsreview.com
ISSN: 1520-0191
July-August 2022 Page No. 788-802
Article History: Received: 30 March 2022, Revised: 8 April 2022, Accepted: 15 April 2022, Publication: 30 April 2022

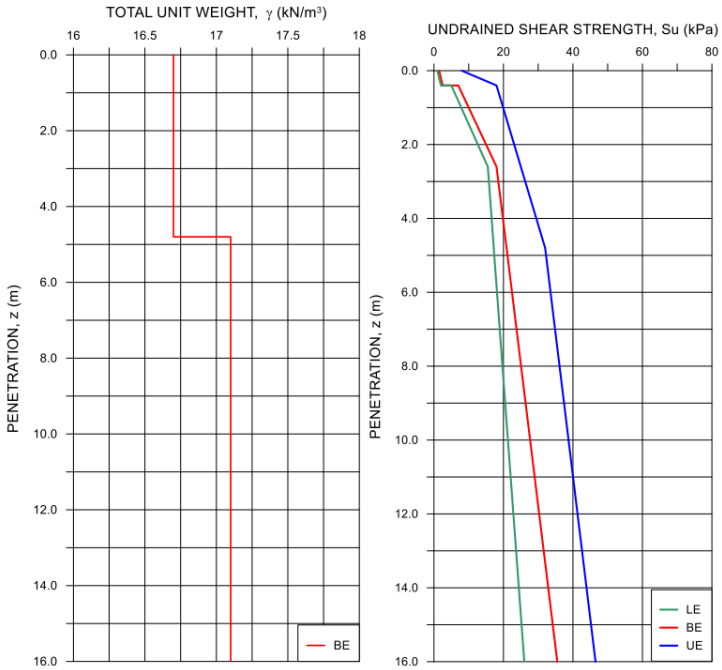

Fig 7: Design soil profile, total unit weight (left) and undrained shear strength (right)

IV. INVERSE CATEARY CALCULATION METHODOLOGY

Mooring system analysis provide the tension load and angle at the mudline point. In agreement with both BV and DNVGL, the mooring loads at anchor padeye need to be considered for the geotechnical design. This is because the tension load reduce and the angle change due to the combined effect of soil bearing and friction resistance of soil on mooring line, taking the form of an inverted catenary. The chain profile and tension distribution will be evaluated with methodology [14] in analogy with [24]. No correction for cyclic and rate effects on soil strength will be considered for chain analysis. In accordance with BV, chain embedment calculations and associated loads and angles at padeye level shall be assessed considering unfactored Lower Estimate (LE) and Upper Estimate (UE) design soil profiles.

Neubecker and Randolph developed analytical expressions that accurately describe the profile and frictional capacity of embedded anchor chain. The detailed equilibrium of a segment of chain is presented schematically in Fig 8. The resistance offered by the soil is Q (per unit length of chain) normal to the chain, and F (per unit length of chain) tangential to the chain.

Forest Chemicals Review
www.forestchemicalsreview.com
ISSN: 1520-0191
July-August 2022 Page No. 788-802
Article History: Received: 30 March 2022, Revised: 8 April 2022, Accepted: 15 April 2022, Publication: 30 April 2022

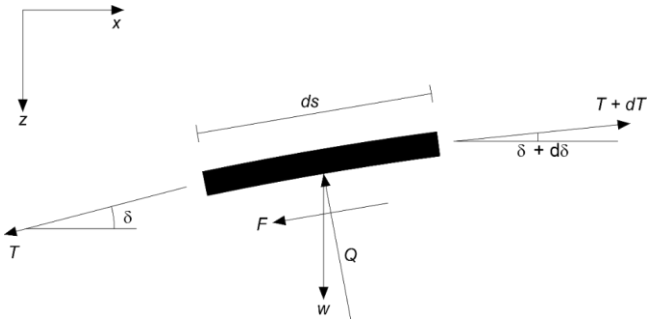

Fig 8: Force Equilibrium of Embedded Chain Element

The differential equations governing the embedded section of the chain are:

$$\frac{dT}{ds} = F + wsin\delta \quad (1)$$

$$T\frac{d\delta}{d\delta} = -Q + wcos\delta \quad (2)$$

where, T tension in the chain; δ angle subtended by the chain to the horizontal; s distance measured along the chain starting at the attachment point; w buoyant weight of the chain per unit length.

Accordingly to Neubecker and Randolph, the soil resistance may be expressed in terms of average normal pressure, q, and friction, f, multiplied by an by an effective width:

$$Q = (E_n d)q \quad (3)$$

$$F = (E_t d)f \quad (4)$$

Where, d nominal chain diameter; E_t, E_n multipliers to give the effective widths in the normal and tangential directions, respectively; E_t and E_n will be taken from table H-2 of DNVGL-RP-E302 [24].

The bearing pressure of the clay was taken as:

$$q = N_c S_u \quad (5)$$

Where, S_u static undrained shear strength of the clay; N_c bearing capacity factor taken from table H-3 of DNVGL-RP-E302 [24];

The friction was approximated as:

$$f = \alpha S_u \quad (6)$$

Where, α friction reduction factor taken from H-4 of DNVGL-RP-E302 [24].

Forest Chemicals Review
www.forestchemicalsreview.com
ISSN: 1520-0191
July-August 2022 Page No. 788-802
Article History: Received: 30 March 2022, Revised: 8 April 2022, Accepted: 15 April 2022, Publication: 30 April 2022

As part of the mooring line installation the chain will be pre-stretched by applying a pretension load. The load will establish an inverse catenary geometry in the buried part of the chain. During operations, the chain will be further stretched and the buried chain length will increase. The difference between the developed buried chain length and the horizontal distance from the padeye to the dip down point will decrease. This will result in additional slack in the non-buried part of the chain. The slack assessment will be performed considering both lower and upper estimate soil profiles for different values of pretension load. The slack was calculated as:

$$S = \left(L_{pre-load} - H_{pre-load}\right) - (L_{design} - H_{design} \tag{7}$$

Where, $L_{pre-load}$ buried chain length due to pre-load; $H_{pre-load}$ horizontal distance from padeye to dip down point due to pre-load; L_{design} buried chain length due to design load; H_{design} horizontal buried chain length due to pre-load.

V. INVERSE CATENARY ANALYZE RESULTS AND DISCUSSION

Under the design mooring loads, the embedded portion of the mooring chain (i.e. the part of the chain comprised between MLP and the padeye) assumes an inverted catenary configuration. The embedded chain profile and tension distribution were evaluated. TABLE VI and TABLE VII show results of inverse catenary analyses in terms of padeye lug loads and angles for BV and DNVGL loading conditions. Inverse catenary analyses were performed using unfactored chain loads at MLP, in order to obtain a realistic estimate of chain configuration (i.e. embedded chain length and load angle at padeye). Padeye loads reported in TABLE VI and TABLE VII were obtained by subtracting the frictional losses along the embedded chain length (determined by inverse catenary analyses) to the factored chain loads at MLP. Inverse catenary analyses were performed for both LE and UE soil conditions, and for both DNVGL and BV design conditions. Embedded chain profiles obtained considering unfactored load at MLP are shown in Fig 9. It can be seen that the load angle at the padeye are significantly influenced by soil conditions. In particular, padeye load angles increase with increasing soil strength and decreasing chain tension, as expected. Computed padeye loads and angles were used as input for holding capacity analyses. Main results of inverse catenary analyses are also summarized in TABLE VIII and TABLE IX, for BV and DNVGL cases respectively. Meanwhile, the main results of the chain soil interaction are reported in TABLE VIII and TABLE IX.

TABLE VI. Factored Loads and Angles at Padeye - BV

Limit State	Mooring Condition	Return Period [yr]	Soil Condition	T_{lug} [kN]	δ_{lug} [°]
Intact Case 2	Intact	100	LE	10,254	21.5
			UE	10,025	30.1
Redundancy	Damaged	100	LE	10,756	18.3

Forest Chemicals Review
www.forestchemicalsreview.com
ISSN: 1520-0191
July-August 2022 Page No. 788-802
Article History: Received: 30 March 2022, Revised: 8 April 2022, Accepted: 15 April 2022, Publication: 30 April 2022

Limit State	Mooring Condition	Return Period [yr]	Soil Condition	T_{lug} [kN]	δ_{lug} [°]
Case			UE	10,489	25.6
Accidental Case	Intact	1,000	LE	11,461	17.8
			UE	11,186	24.8

TABLE VII. Factored Loads and Angles at Padeye - DNVGL

Limit State	Mooring Condition	Return Period [yr]	Soil Condition	T_{lug} [kN]	δ_{lug} [°]
ULS	Intact	100	LE	11,956	19.9
			UE	11,710	27.8
ALS	Damaged	100	LE	12,987	16.8
			UE	12,687	23.5
ALS	Intact	1,000	LE	14,075	16.2
			UE	13,761	22.7
Sensitivity	Intact	1	LE	4,213	37.8
			UE	4,082	53.5

TABLE VIII. Main Results of the Chain Soil Interaction – BV

Limit State	Mooring Condition	Return Period [yr]	Soil Condition	Tmudline [kN]	Buried Chain Length [m]	Horizontal Buried Chain Projection [m]
Intact Case 2	Intact	100	LE	8,016	69.54	68.24
			UE		48.99	47.33
Redundancy Case	Damaged	100	LE	10,895	78.06	76.86
			UE		55.66	54.16
Accidental Case	Intact	1,000	LE	11,585	79.88	78.70
			UE		57.10	55.63

TABLE IX. Main Results of the Chain Soil Interaction - DNVGL

Limit State	Mooring Condition	Return Period [yr]	Soil Condition	Tmudline [kN]	Buried Chain Length [m]	Horizontal Buried Chain Projection [m]
ULS	Intact	100	LE	9,304	73.56	72.32

Forest Chemicals Review
www.forestchemicalsreview.com
ISSN: 1520-0191
July-August 2022 Page No. 788-802
Article History: Received: 30 March 2022, Revised: 8 April 2022, Accepted: 15 April 2022, Publication: 30 April 2022

			UE		52.12	50.54
ALS	Damaged	100	LE	12,898	80.58	79.42
			UE		59.70	58.28
ALS	Intact	1,000	LE	13,828	81.44	80.30
			UE		61.45	60.06
Sensitivity	Intact	1	LE	2,730	46.28	44.40
			UE		31.61	29.08

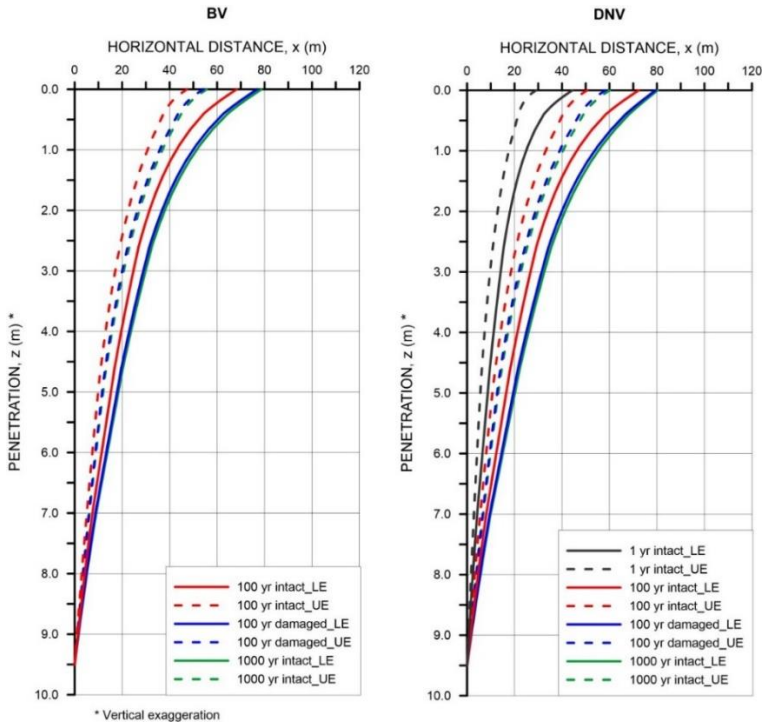

Fig 9: Buried chain profile results for BV (left) and DNVGL (right)

The slack assessment was performed in accordance with considering both lower and upper estimate soil profiles. In the absence of specific value of load pretension, the evaluation of slack has been performed for different values of horizontal pulling load at mudline. With reference to Fig 10 the calculated slack (movement of chain along seabed from pretension to max intact load) is expected to be in the range 2.3 m - 0.4 m dependent on soft or stiff soil conditions and on installation (pretension) load. This calculation was carried out under the assumption that reference condition for the slack was the DNVGL Case ALS 1000 yrs Intact.

Forest Chemicals Review
www.forestchemicalsreview.com
ISSN: 1520-0191
July-August 2022 Page No. 788-802
Article History: Received: 30 March 2022, Revised: 8 April 2022, Accepted: 15 April 2022, Publication: 30 April 2022

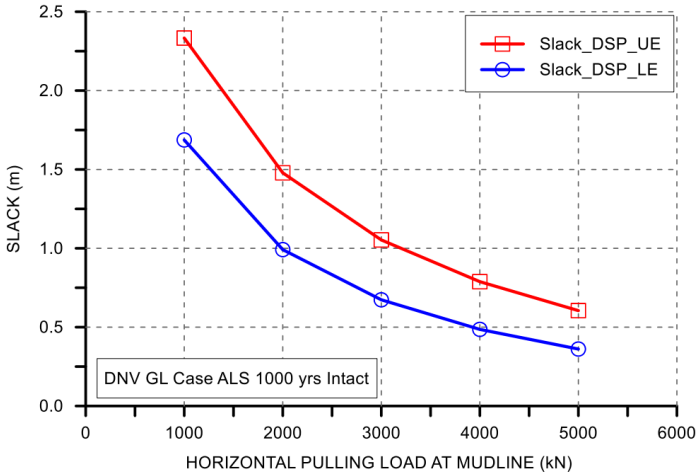

Fig 10: Slack - DNVGL Case ALS 1000 yrs Intact

VI. CONCLUSIONS

The turret mooring system of a deepwater oilfield development project in the South China Sea is taken as the research object, and the mechanical modeling, mooring load combination, seabed soil characteristics analysis and final engineering calculation of the suction pile inverse catenary are investigated. The following conclusions are drawn:

(1). Based on the theory of soil mechanics, a complete engineering model of suction pile inverse catenary was established as per the force control unit of the inverse catenary. The calculation formula of the mooring lug load and angle of the suction pile and the interaction of chain soil was obtained, and the calculation method of the inverse catenary slack was proposed.

(2). According to the development of a deepwater oil field in the South China Sea, the characteristics of the FPSO turret mooring system were analyzed, the mooring analysis conditions were combined as per BV and DNVGL rules, and so as to determine the final inverse catenary engineering seabed loads. Meanwhile, the seabed geological survey data of mooring area are analyzed, and the total weight and undrained shear strength of the designed soil profile are obtained to provide input parameters for the design of the reverse catenary.

(3). In the design and checking conditions, the tension range of the suction pile inverse catenary of this FPSO mooring is 10254kN~14075kN, the lug load angle range is 16.2° ~30.1° , and the horizontal projection distance of the embedded chain range is 47.33m~80.30m. It can also be seen that the calculation results of BV rule and DNV rule are relatively close, the results based on different rules are mutually verified.

Forest Chemicals Review
www.forestchemicalsreview.com
ISSN: 1520-0191
July-August 2022 Page No. 788-802
Article History: Received: 30 March 2022, Revised: 8 April 2022, Accepted: 15 April 2022, Publication: 30 April 2022

(4). The calculated slack (movement of chain along seabed from pretension to max intact load) is expected to be in the range 2.3 m - 0.4 m dependent on soft or stiff soil conditions and on installation (pretension) load.

DECLARATION

Conflict of Interest: We declare that they have no conflict of interest.

Ethical approval: This article does not contain any studies with human participants or animals performed by any of the authors.

Informed consent: Informed consent was obtained from all individual participants included in the study.

ACKNOWLEDGEMENTS

This work was supported by Science and Technology R&D Projects of China National Offshore Oil Corporation (CNOOC) [grant number CNOOC-KJ 135 JSPJ 08 GC 2019-02]. The first author are greatly grateful to the referees for their helpful comments and suggestions, which help improve this paper.

REFERENCES

[1] CNOOC. FPSO and single point mooring system design. Guidelines for offshore oil engineering design. Petroleum Industry Press, Beijing, 2007.
[2] Meng H X, Kloul L, Rauzy A (2018) Production Availability Analysis of Floating Production Storage and Offloading (FPSO) Systems. Applied Ocean Research 74: 117-126.
[3] Luo Yong, Wang Hongwei, Yan Fasuo. Design and Analysis of Station Keeping System for Floating Structures. Haerbin: Harbin Engineering University Press, 2015.
[4] Ma K T, Luo Y, Thomas K, Wu Y Y. Mooring System Engineering for Offshore Structures. Houston: Gulf Professional Publishing, 2019.
[5] Wu J, Lu, D D, Yao X and Wu J (2020) Technology review of FPSO turret field. Ship Engineering 42: 113-119,148.
[6] LI D, BAI X P, YI C (2016) Selection and design on single point mooring system of HYSY118 FPSO. Ship &Ocean Engineering 45: 166-171.
[7] Du Q G, Shen X C, Tan G R, Liu C and Fu D M (2017) Priliminary Study on Development and Application of FPSO. Ocean Engineerng Equipment and Technology 4: 63-68.
[8] MARIC (2021) HYSY119 FPSO, The Pillars of a Great Power. Ship & Boat 32: 120-123.
[9] Yan J, Qiao D Q, Fan T H and Ou J P (2016). Concept Design of Deepwater Catenary Mooring Lines with Submerged Buoy. “The Twelfth ISOPE Pacific/Asia Offshore Mechanics Symposium”. Available at https://onepetro.org/ISOPEPACOMS/proceedings-abstract/PACOMS16/All-PACOMS16/ISOPE-P-16-013/25945. Accessed April 2022

Forest Chemicals Review
www.forestchemicalsreview.com
ISSN: 1520-0191
July-August 2022 Page No. 788-802
Article History: Received: 30 March 2022, Revised: 8 April 2022, Accepted: 15 April 2022, Publication: 30 April 2022

[10] Liu H X, Li Z, Zhang Y M (2018) Offshore Geotechnical Problems in Deepwater Mooring Techniques for Large Floating Structures. American Journal of Engineering and Applied Sciences 11:598-610.

[11] Claudia Rendón-Conde, Ernesto Heredia-Zavoni (2014) Predictive reliability assessment of suction caissons for moored floating systems. Ocean Engineering 88: 499‑507.

[12] Agarwal A K, Jain A K (2003) Nonlinear coupled dynamic response of offshore Spar platforms under regular sea waves. Ocean Engineering 30: 517-551.

[13] Koo B J, Kim M H, Randall R E (2004) Mathieu instability of a Spar platform with mooring and risers. Ocean Engineering 31: 2175-2208.

[14] Neubecker S R, Randolph M F (1995). Performance of Embedded Anchor Chains and Consequences for Anchor Design. "Offshore Technology Conference". 1995: Available at https://onepetro.org/OTCONF/proceedings-abstract/95OTC/All-95OTC/OTC-7712-MS/43835. Accessed April 2022

[15] Hong Y P, Lee D Y, Choi Y H, Hong S H, Kim S E (2005). An experimental study on the extreme motion responses of a Spar platform in the heave resonant waves. "Proceeding of the 15th International Offshore and Polar Engineering Conference".

[16] Montasir O A, Kurian V J (2011) Effect of slowly varying drift forces on the motion characteristics of Truss Spar platforms. Ocean Engineering 38: 1417-1429.

[17] Zhang R, Tang Y, Hu J, et al (2013) Dynamic response in frequency and time domains of a floating foundation for offshore wind turbines. Ocean Engineering 60: 115-123.

[18] Zhang F, Yang J M, Li R P (2007) Numerical research on hydrodynamics of a new cell-truss Spar platform. The Ocean Engineering 25: 1-8.

[19] Ying W, Yang J, Hu Z, et al (2008) Theoretical research on hydrodynamics of a geometric Spar in frequency and time-domains. Journal of Hydrodynamics, Ser. B 20: 30-38.

[20] Zhao Y B, Liu H X (2015) The drag effects on the penetration behavior of drag anchors during installation. The Ocean Engineering 109:169-180.

[21] Hou H M, Dong G H, Xu T J et al (2018) Dynamic Analysis of Embedded Chains in Mooring Line for Fish Cage System. Polish Maritime Research 25: 83 - 97.

[22] BV NR 493 DT R03 E- Rule Note, Classification of Mooring Systems for Permanent and Mobile Offshore Units, 2015.

[23] DNVGL-OS-E301- Offshore Standard, Position Mooring, 2015.

[24] DNVGL-RP-E302- Recommended Practice, Design and installation of plate anchors in clay, 2017.